August 23, 2012

Ultrashort pulses and short-pulse equations in 2+1 dimensions

Y. Shen
N. Whitaker
Panos Kevrekidis, *UMASS, Amherst*
N. L. Tsitsas
D. J. Frantzeskakis

Ultrashort pulses and short-pulse equations in 2 + 1 dimensions

Y. Shen,[1] N. Whitaker,[1] P. G. Kevrekidis,[1] N. L. Tsitsas,[2] and D. J. Frantzeskakis[3]
[1]*Department of Mathematics and Statistics, University of Massachusetts, Amherst, Massachusetts 01003-4515, USA*
[2]*Department of Informatics, Aristotle University of Thessaloniki, GR-54124 Thessaloniki, Greece*
[3]*Department of Physics, University of Athens, Panepistimiopolis, Zografos, Athens 15784, Greece*
(Received 4 June 2012; published 23 August 2012)

In this paper, we derive and study two versions of the short pulse equation (SPE) in $(2+1)$ dimensions. Using Maxwell's equations as a starting point, and suitable Kramers-Kronig formulas for the permittivity and permeability of the medium, which are relevant, e.g., to left-handed metamaterials and dielectric slab wave guides, we employ a multiple scales technique to obtain the relevant models. General properties of the resulting $(2+1)$-dimensional SPEs, including fundamental conservation laws, as well as the Lagrangian and Hamiltonian structure and numerical simulations for one- and two-dimensional initial data, are presented. Ultrashort one-dimensional breathers appear to be fairly robust, while rather general two-dimensional localized initial conditions are transformed into quasi-one-dimensional dispersing wave forms.

DOI: 10.1103/PhysRevA.86.023841 PACS number(s): 42.65.Tg, 42.65.Re, 05.45.Yv

I. INTRODUCTION

Ultrashort pulses, having a duration of a few optical cycles, have been the subject of intense study over the past years; this is due to the fact that they find many applications in various contexts, ranging from light-matter interactions, harmonic generation, attosecond physics, nonlinear optics, and others [1]. A theme of particular interest related to ultrashort pulses, is their evolution in nonlinear media characterized by an intensity-dependent refractive index. In that respect, models describing ultrashort pulses in nonlinear media, as well as their systematic study, have attracted much attention; see, e.g., Refs. [2–9]. Prominent examples are the modified Korteweg-de Vries (mKdV) equation [3], the sine-Gordon (sG) equation [5,6], and combined mKdV-sG equations [7–9] among others. Note that most of these works refer to the one-dimensional (1D) setting; in the two-dimensional (2D) one, pertinent studies are related to few-cycle solitons described by the generalized Kadomtsev-Petviashvilli (KP) equation [10] and collapse dynamics of ultrashort spatiotemporal pulses [11].

Another model describing ultrashort pulse dynamics is the so-called short-pulse equation (SPE), which was first derived in the context of nonlinear fiber optics [12] and later in the context of nonlinear metamaterials [13]. From the physical point of view, the interest in the SPE model arises from the fact that its few-cycle pulse solutions have been shown to compare more favorably to the ones of the original Maxwell's equations, as compared to pertinent solutions of the more traditional nonlinear Schrödinger (NLS) model [12,14]. Furthermore, this model is also interesting from a mathematical point of view, due to the existence of an infinite hierarchy of conserved quantities [15], its connection to the sG model and, thus, to its complete integrability [16]. The SPE admits various types of solutions, including singular soliton solutions—the so-called loop solitons [17]—as well as other nonsingular solutions, such as peakons, breather- and periodic-type wave forms [13,17–19]. Note that, recently, wave-breaking phenomena [20], as well as the global well-posedness question [21] of the SPE, were also investigated. The above volume of work refers to the 1D setting; to the best of our knowledge, the SPE has not been considered or analyzed so far in 2D.

In this work, we derive and study two different versions of the SPE in $(2+1)$ dimensions, namely the SPE-I and SPE-II. In particular, starting from Maxwell's equations, and assuming general Kramers-Kronig or Sellmeier formulas for the permittivity and permeability (see, e.g., Ref. [22]), we use a multiscale expansion method to obtain the SPE-I and SPE-II models. Then, we study the general properties of each model, present the Hamiltonian, Lagrangian, and momenta, and also obtain zero-mass constraints that are used in the simulations (and, specifically, in the preparation of the initial data). Next, we explore the dynamics of ultrashort pulses in 2D, employing as initial conditions either the breather solution of the underlying 1D SPE or a wave form localized in 2D; our purpose is to investigate if ultrashort pulses are prone to transverse instabilities (induced by the presence of diffraction in our models) and also identify purely 2D structures that can be supported by the SPE-I and SPE-II. We find that the 1D breathers are stable in the 2D setting, while 2D initial data are gradually transformed into quasi-1D wave forms, reminiscent of the 1D solutions.

Our presentation is structured as follows. In Sec. II, we derive the SPE-I and SPE-II models. Sections III and IV are devoted to the general properties and numerical study of SPE-I and SPE-II, respectively. Finally, in Sec. V, we summarize and discuss our conclusions.

II. DERIVATION OF 2D SHORT-PULSE EQUATIONS

We consider the propagation of TE_z (transverse-electric field propagating along the z axis) electromagnetic (EM) waves in a planar metamaterial or optical waveguide structure. In particular, we consider the case where the electric and magnetic field components take the form $\mathbf{E}(x,z,t) = \hat{\mathbf{y}} E_y(x,z,t)$ and $\mathbf{H}(x,z,t) = \hat{\mathbf{x}} H_x(x,z,t) + \hat{\mathbf{z}} H_z(x,z,t)$, where $\hat{\mathbf{x}}, \hat{\mathbf{y}}, \hat{\mathbf{z}}$ are the unit vectors along the x, y, z directions, respectively, and we have assumed no variations (i.e., a homogeneous medium) with respect to the variable y. Under these assumptions, we may use Maxwell's equations—namely, Ampére's and Faraday's

laws—take, respectively, the following form:

$$-\frac{\partial H_z}{\partial x}+\frac{\partial H_x}{\partial z}=\frac{\partial D_y}{\partial t}, \tag{1}$$

$$\frac{\partial E_y}{\partial z}=\frac{\partial B_x}{\partial t}, \quad \frac{\partial E_y}{\partial x}=-\frac{\partial B_z}{\partial t}. \tag{2}$$

Here D_y is the y component of the displacement vector $\mathbf{D}=\hat{\mathbf{y}}D_y$. Furthermore, we assume that the magnetic induction vector $\mathbf{B}$ is connected with the magnetic field intensity $\mathbf{H}$ by means of the constitutive relation $\hat{\mathbf{B}}=\hat{\mu}(\omega)\hat{\mathbf{H}}$, where $\hat{\mu}(\omega)$ is the linear magnetic permeability (hereafter, we use f and $\hat{f}$ to denote any function f in the time and frequency domain, respectively). Additionally, we assume that the considered structure exhibits a weak cubic (Kerr-type) nonlinearity in its dielectric response. In other words, $D_y=\epsilon * E_y+P_{NL}$, where ϵ is the permittivity, $*$ denotes the convolution integral $f(t)*g(t)=\int_{-\infty}^{+\infty}f(\tau)g(t-\tau)d\tau$ of any functions $f(t)$ and $g(t)$, while the nonlinear polarization P_{NL} is of the form

$$P_{NL}=\epsilon_0\int_{-\infty}^{+\infty}\chi_{NL}(t-\tau_1,t-\tau_2,t-\tau_3)\times E_y(\tau_1)E_y(\tau_2)E_y(\tau_3)d\tau_1d\tau_2d\tau_3. \tag{3}$$

Here, ϵ_0 is the dielectric constant of vacuum and χ_{NL} is the nonlinear electric susceptibility of the medium. In the case of small-amplitude, *ultrashort* pulse propagation, the nonlinear response can safely be considered to be *instantaneous*, namely,

$$\chi_{NL}(t-\tau_1,t-\tau_2,t-\tau_3)=\kappa\delta(t-\tau_1)\delta(t-\tau_2)\delta(t-\tau_3), \tag{4}$$

where κ is the Kerr coefficient given by $\kappa=\pm E_c^{-2}$, with E_c being a characteristic electric field value; generally, both cases of focusing ($\kappa>0$) and defocusing ($\kappa<0$) dielectrics are possible. Notice that Eqs. (3) and (4) imply that $P_{NL}=\epsilon_0\kappa E_y^3$ and, thus, $D_y=\epsilon * E_y+\epsilon_0\kappa E_y^3$. Substituting the considered form of the constitutive relations into Eqs. (1) and (2), we derive the following equation for the y component of the electric field intensity (E_y) which, for convenience, will be denoted hereafter by E:

$$\nabla^2E-\partial_t^2(\epsilon*\mu*E)-\epsilon_0\kappa\partial_t^2(\mu*E^3)=0, \tag{5}$$

where $\nabla^2\equiv\partial_x^2+\partial_z^2$ is the Laplacian in the (x,z) plane.

Equation (5) is the $(2+1)$-dimensional generalization of the 1D Klein-Gordon type model derived in the context of nonlinear fiber optics [12,23] (in this case, $\mu=$ const) and nonlinear metamaterials [13,24–26] (in this case, $\partial_\omega\hat{\mu}\neq 0$). Below, we will analyze the latter (more general) case, and assume that both permittivity and permeability are frequency dependent. In particular, considering general Kramers-Kronig or Sellmeier formulas (see, e.g., Ref. [22]), we assume that the frequency dependence of $\hat{\epsilon}\equiv\hat{\epsilon}(\omega)$ and $\hat{\mu}\equiv\hat{\mu}(\omega)$ can be approximated by the relations

$$\hat{\epsilon}(\omega)\approx\epsilon_0\left(\alpha_1-\frac{\alpha_2}{\omega^2}\right), \quad \hat{\mu}(\omega)\approx\mu_0\left(\beta_1-\frac{\beta_2}{\omega^2}\right), \tag{6}$$

where $\alpha_1,\alpha_2,\beta_1$, and β_2 are some constants. The above approximations can be applied to the contexts of nonlinear left-handed metamaterials and nonlinear optical slab waveguides. Specifically, in the context of nonlinear left-handed metamaterials, $\alpha_1=1$, $\alpha_2=\omega_p^2$, $\beta_1=1-F$, and $\beta_2=F\omega_{\rm res}^2$, where ω_p, F, and $\omega_{\rm res}$ denote, respectively, the plasma frequency, the filling factor, and the magnetic permeability resonance frequency [13]. On the other hand, in the context of nonlinear optical slab waveguides, $\alpha_1=\epsilon_r^{(0)}$, $\alpha_2=\epsilon_r^{(2)}$, $\beta_1=1$, and $\beta_2=0$, where $\epsilon_r^{(0)}$ and $\epsilon_r^{(2)}$ are relative dielectric constants (with $\epsilon_r^{(2)}$ being measured in units of squared angular frequency) obtained by matching the full form of the permittivity with the first of Eqs. (6) over a specific wavelength range in the infrared regime [12].

Next, we express Eq. (5) in the frequency domain and substitute Eqs. (6), keeping terms up to order $\mathcal{O}(\omega^{-2})$ (i.e., assuming that $\alpha_1\beta_2/\omega^4\ll 1$); then, expressing the resulting equation back in time domain, and measuring time, space, and field intensity E^2 in units of $1/\sqrt{\alpha_2}$, $c/\sqrt{\alpha_1\alpha_2\beta_1}$, and $|\kappa|^{-1}$, respectively, we reduce Eq. (5) to the following dimensionless form:

$$\nabla^2E-\partial_t^2E-\alpha E-s_\kappa\left(\beta E^3+\gamma\partial_t^2E^3\right)=0. \tag{7}$$

In the above equation, $s_\kappa=\mathrm{sgn}(\kappa)$, while the other constants are given by

$$\alpha=\frac{1}{\alpha_1}+\frac{\beta_2}{\alpha_2\beta_1}, \quad \beta=\frac{\beta_2}{\alpha_1\alpha_2\beta_1}, \quad \gamma=\frac{1}{\alpha_1}. \tag{8}$$

Note that in the context of nonlinear metamaterials $\alpha=1+\beta=1+F\omega_{\rm res}^2/[(1-F)\omega_p^2]$ and $\gamma=1$, while in the context of nonlinear optical slab waveguides $\alpha=\gamma=1/\epsilon_r^{(0)}$ and $\beta=0$.

We now consider propagation of ultrashort pulses, of width ε, where $0<\varepsilon\ll 1$ is a formal small parameter, which will also set the field amplitude (see below). Then, we employ the method of multiple scales to derive from Eq. (7) two different versions of short pulse equations in $(2+1)$ dimensions. In that regard, we introduce the following asymptotic expansion for the unknown field E:

$$E=\varepsilon E_1(T,X_n,Z_n)+\varepsilon^2E_2(T,X_n,Z_n)+\cdots, \tag{9}$$

where the functions E_n depend on the spatial variables X_n and Z_n ($n=1,2,\ldots$), as well as on the fast time variable T. Defining Z_n as

$$Z_n=\varepsilon^n z, \tag{10}$$

we consider two different definitions for X_n and T, namely

$$X_n=\varepsilon^{n-1}x, \quad T=\frac{t-z}{\varepsilon}, \tag{11}$$

$$X_n=\varepsilon^n x, \quad T=\frac{t-(x+z)/\sigma\sqrt{2}}{\varepsilon}, \tag{12}$$

where $\sigma=\pm 1$. Then, substituting Eqs. (9), (10), and (11) in Eq. (7), we derive at order $\mathcal{O}(\varepsilon)$ the following $(2+1)$-dimensional SPE for the unknown field E_1:

$$2\frac{\partial^2E_1}{\partial Z_1\partial T}-\frac{\partial^2E_1}{\partial X_1^2}+\alpha E_1+s_\kappa\gamma\frac{\partial^2}{\partial T^2}\left(E_1^3\right)=0. \tag{13}$$

Equation (13) will be called hereafter SPE-I. Similarly, substituting Eqs. (9), (10), and (12) in Eq. (7), we derive [again at order $\mathcal{O}(\varepsilon)$] another $(2+1)$-dimensional version of the SPE, namely

$$2\sigma\left(\frac{\partial^2E_1}{\partial Z_1\partial T}+\frac{\partial^2E_1}{\partial X_1\partial T}\right)+\alpha E_1+s_\kappa\gamma\frac{\partial^2}{\partial T^2}\left(E_1^3\right)=0, \tag{14}$$

which will be called hereafter SPE-II. We note that variants of these models have been considered in the past in the context of ultrashort propagation in nonlinear dielectrics [2,4], and more recently in relevant studies [9], as well as in the context of collapse in two-level media [11].

III. SPE-I: GENERAL PROPERTIES AND NUMERICAL STUDY

In this section, we focus on the SPE-I which, for simplicity of notation, is expressed in the form

$$2E_{zt} - E_{xx} + \alpha E + s(E^3)_{tt} = 0, \tag{15}$$

where $s = s_\kappa \gamma$ and subscripts denote partial derivatives, with z being the evolution variable. Below, we will consider general properties of this equation and discuss its solutions.

A. Properties and canonical structure

First, we study the Hamiltonian structure of Eq. (15). For this purpose, we integrate Eq. (15) with respect to time t and, introducing the auxiliary field $E = \phi_t$, we express Eq. (15) as follows:

$$2\phi_{tz} - \phi_{xx} + \alpha\phi + s(\phi_t^3)_t = 0. \tag{16}$$

Then, it can be verified that Eq. (16) can be obtained from the variational principle, with Lagrangian density:

$$\mathcal{L} = -\frac{\alpha}{2}\phi^2 + \frac{s}{4}\phi_t^4 + \phi_t\phi_z - \frac{1}{2}\phi_x^2. \tag{17}$$

From this Lagrangian density, we can derive the Hamiltonian

$$\begin{aligned} H &= \int_{-\infty}^{+\infty}\int_{-\infty}^{+\infty}\left(\frac{\partial\mathcal{L}}{\partial\phi_z}\phi_z - \mathcal{L}\right)dt\,dx \\ &= \int_{-\infty}^{+\infty}\int_{-\infty}^{+\infty}\left(\frac{\alpha}{2}\phi^2 - \frac{s}{4}\phi_t^4 + \frac{1}{2}\phi_x^2\right)dt\,dx, \end{aligned} \tag{18}$$

as well as the momenta

$$M_t = \int_{-\infty}^{+\infty}\int_{-\infty}^{+\infty}\frac{\partial\mathcal{L}}{\partial\phi_z}\phi_t dt\,dx = \int_{-\infty}^{+\infty}\int_{-\infty}^{+\infty}\phi_t^2 dt\,dx, \tag{19}$$

$$M_x = \int_{-\infty}^{+\infty}\int_{-\infty}^{+\infty}\frac{\partial\mathcal{L}}{\partial\phi_z}\phi_x dt\,dx = \int_{-\infty}^{+\infty}\int_{-\infty}^{+\infty}\phi_t\phi_x dt\,dx. \tag{20}$$

Let us next consider the Fourier transform of Eq. (15) with respect to time t, which leads to the equation

$$(i\omega)\hat{E}_z = \frac{1}{2}\hat{E}_{xx} - \frac{\alpha}{2}\hat{E} - \frac{s}{2}(i\omega)^2\hat{E}^3. \tag{21}$$

The above equation implies that

$$\hat{E}_z(\omega_t,x,z) = -\frac{i}{2}\left(\frac{\hat{E}_{xx} - \alpha\hat{E}}{\omega} + s\omega\hat{E}^3\right), \quad \text{for} \quad \omega \neq 0, \tag{22}$$

$$\hat{E}_{xx} - \alpha\hat{E} = 0, \quad \text{for} \quad \omega = 0. \tag{23}$$

In our numerical simulations below, we will set $\hat{E}(\omega = 0,x,z) = 0$, so that Eq. (23) is satisfied. Thus, in this case, the Fourier transform of the field E leads to the following "zero-mass constraint:"

$$\int_{-\infty}^{\infty} E(t,x,z)dt = 0 \quad \text{for any} \quad x,z, \tag{24}$$

which also holds for the traditional SPE in $(1+1)$ dimensions (see, e.g., the relevant analysis of Ref. [27]).

B. 1D breatherlike structures

Let us now seek one-dimensional (1D) solutions of Eq. (15), by assuming that the unknown field E depends on the traveling-wave coordinates ξ and η, defined as

$$\xi = z, \quad \eta = t + cx + \frac{c^2}{2}z, \tag{25}$$

where c is an arbitrary real constant setting the velocities of the traveling wave in the (x,t) and (x,z) planes. Using the above variables, Eq. (15) is reduced to the form

$$2E_{\xi\eta} + \alpha E + s(E^3)_{\eta\eta} = 0, \tag{26}$$

which is actually the $(1+1)$-dimensional SPE [12]. As shown in the simulations of Ref. [18], the most robust among the various solutions of the 1D SPE is the breatherlike structure (this solution satisfies the zero-mass constraint). Naturally, this purely 1D structure satisfies the full 2D SPE-I, Eq. (15) and, thus, an interesting question concerns the stability of this solution in the 2D space. A similar question appears in many physically relevant models and, in many cases, the answer is that such "planar" solutions are prone to transverse instabilities in higher-dimensional settings; as characteristic examples, we mention the line soliton solutions of the Kadomtsev-Petviashvilli-I (KP-I) equation which decay into lumps [28,29], or the dark soliton stripes of the defocusing NLS equation which decay into vortices [30,31] in $(2+1)$ dimensions.

To study the stability of the 1D breatherlike solution of Eq. (26) in the framework of the full 2D SPE-I, we have used the following procedure. We employed the breather solution of the 1D SPE Eq. (26) and also added, as a perturbation, a small noisy signal, of amplitude of 1% of the breather's amplitude. Then, using the resulting structure (cf. top left panel of Fig. 1) as an initial condition, we numerically integrated Eq. (15) by means of a Galerkin method (and assuming periodic boundary conditions in our numerical scheme). The results (corresponding to parameter values $c = 0$, $s = -1/3$, and $\alpha = -2$) are shown in the panels of Fig. 1, in terms of different contour plots depicting the profile of the 1D breather in the (x,t) plane for various values of the propagation distance z [and also the evolution at $x = 0$ as a function of (z,t)]. It is clear that the breather is robust, at least up to $z = 200$ (where the simulation ended). We should also mention that, for these simulations, we have also calculated the evolution of the Hamiltonian and momenta [cf. Eqs. (18)–(20)]. The results, depicted in Fig. 2, justify the conservation of these quantities with a satisfactory (relative) accuracy, of order 10^{-3} or less.

We finally note that similar results (not shown here) were also obtained for breathers with, i.e., for $c \neq 0$ in Eq. (25); in such a case, the only difference is that the breather is "tilted," i.e., oblique in the (x,t) plane with respect to its direction in the case $c = 0$ and follows a similar evolution (i.e., it is stable up to the end of the simulation time).

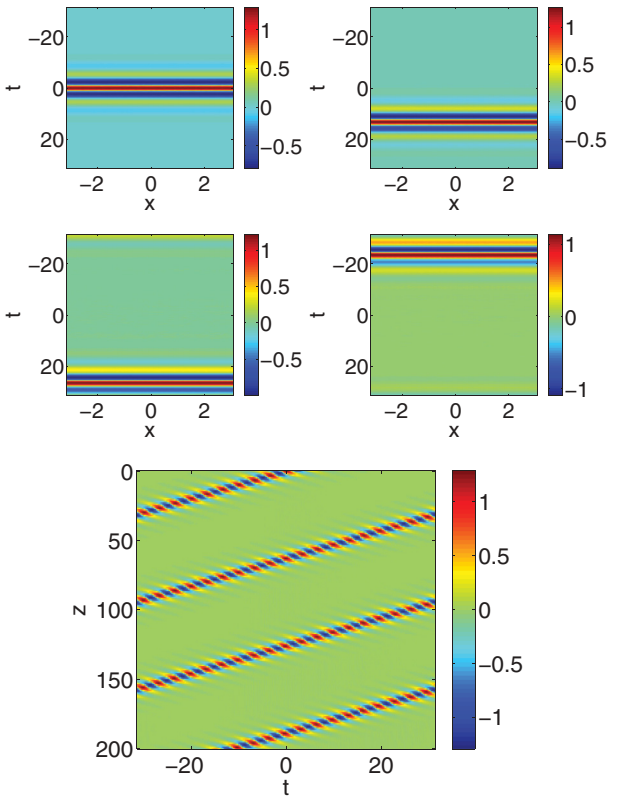

FIG. 1. (Color online) Top (four) panels: contour plots showing profiles of the evolution of a perturbed 1D breather in the (x,t) plane, when evolved according to Eq. (15). Snapshots correspond to $z = 0$ (top left), $z = 50$ (top right), $z = 100$ (bottom left), and $z = 150$ (bottom right). Bottom panel: the evolution of the breather for $x = 0$. Parameter values are $c = 0$, $s = -1/3$, and $\alpha = -2$. All depicted quantities are dimensionless.

C. Localized initial data

Having discussed the properties of the 1D breather in the 2D setting, we now turn our attention to initial data associated with Eq. (26), which are localized in both transverse directions, x and t. In that regard, it is convenient to consider at first the decomposition $E(x,t) = f(t)g(x)$, and substitute this ansatz in the zero-mass constraint, Eq. (24). This way, for nontrivial solutions, we derive the necessary condition $\int_{-\infty}^{\infty} f(t)dt = 0$.

Taking into account the above constraint, we now may use $f(t) = (1 - t^2)\exp(-t^2/2)$ which has the above property, and also choose $g(x)$ to be of the same functional form, namely, $g(x) = (1 - x^2)\exp(-x^2/2)$. The aim of the latter choice is to produce a two-dimensional localized wave form. Employing these choices, we can now numerically integrate Eq. (15), using the initial condition:

$$E(z = 0,x,t) = (1 - x^2)(1 - t^2)\exp[-(x^2 + t^2)/2]. \quad (27)$$

The results of our simulations are presented in Fig. 3, where we show the evolution of this initial data. It is clearly observed that, already at small values of the propagation distance ($z \approx 2$), the initially localized structure bends and splits at $(x,t) = (0,0)$, thus forming two "winglike" structures. The size (length) of these structures is small at the early stages of the evolution but, afterward, their spatial extent is increased, as the initial data progressively disperses. This way, the resulting

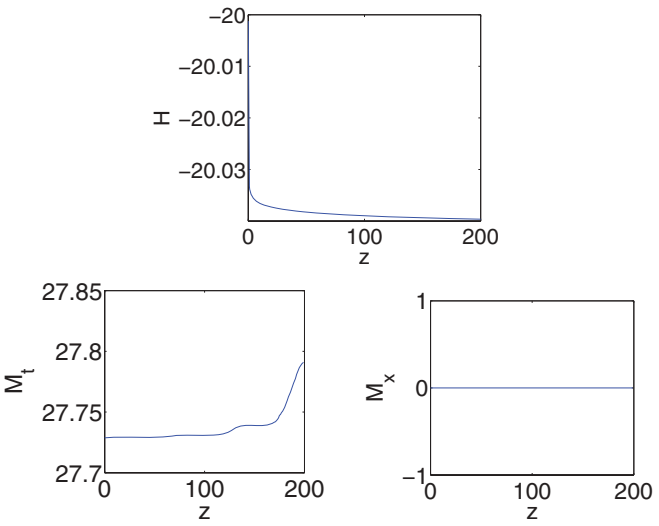

FIG. 2. (Color online) Evolution of the conserved quantities of the SPE-I for the simulation shown in Fig. 1: top panel shows the Hamiltonian H and bottom panels show the momenta M_t (left) and M_t (right). The relative error for H and M_t is of order 10^{-4} and 10^{-3}, respectively, and M_x is zero. All depicted quantities are dimensionless.

structures yield, at longer propagation distances (see bottom panels of Fig. 3), a quasi-one-dimensional pattern, somewhat reminiscent of the breather states examined previously. Here we should mention that our simulations end up at relatively small distance ($z = 38$) in order to avoid interference of these

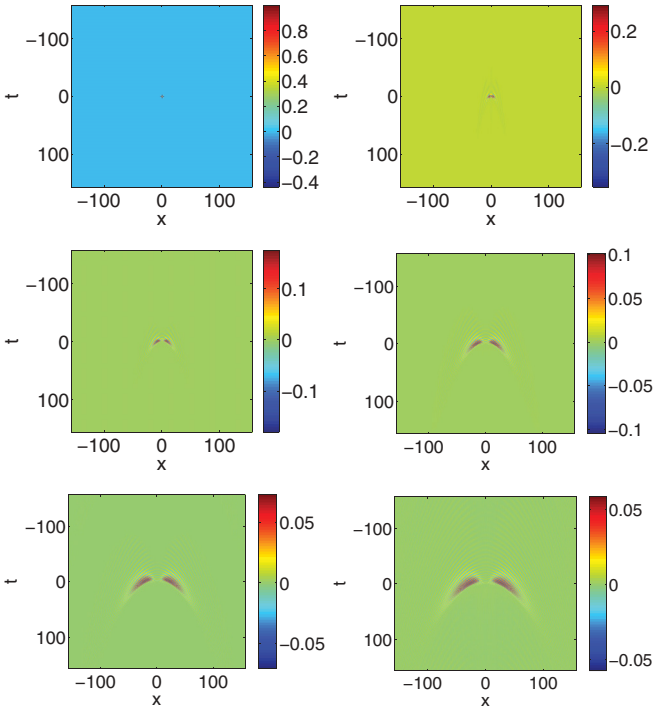

FIG. 3. (Color online) Contour plots showing profiles of the field E, in the (x,t) plane, evolved as per SPE-I, Eq. (15), with localized initial data [cf. Eq. (27)]. The snapshots, from left to right, and top to bottom correspond to $z = 0,3,10,20,30,38$. Parameter values are $s = -1/3$ and $\alpha = -2$. All depicted quantities are dimensionless.

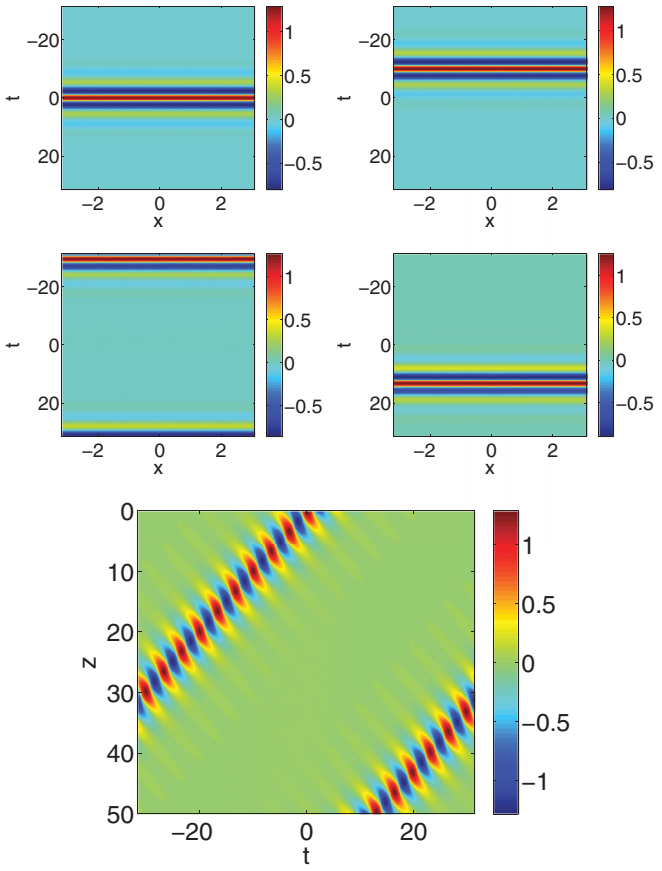

FIG. 4. (Color online) Top (four) panels: contour plots showing profiles of the 1D breather solution of Eq. (38) in the (x,t) plane, when evolved as per Eq. (28). Snapshots correspond to $z = 0$ (top left), $z = 10$ (top right) $z = 30$ (bottom left), and $z = 50$ (bottom right). Bottom panel: the evolution of the breather for $x = 0$. Parameter values are $c = 0$, $s = -1/3$, $\alpha = -2$, and $\sigma = 1$. All depicted quantities are dimensionless.

expanding quasi-1D structures with the boundaries (recall that we use periodic boundary conditions in our numerical scheme).

We also note in passing that we have tried other localized initial conditions, which led to qualitatively similar results: in all cases, the respective evolutions of the initial localized data gradually transformed into quasi-one-dimensional dispersing structures of the above type.

IV. SPE-II: GENERAL PROPERTIES AND NUMERICAL STUDY

Let us now consider the SPE-II which we express, for simplicity of notation, in the following form:

$$2\sigma(E_{zt} + E_{xt}) + \alpha E + s(E^3)_{tt} = 0, \tag{28}$$

where $s = s_\kappa \gamma$, as in the SPE-I. Below we will follow the presentation of the previous section and discuss general properties of this model, such as the corresponding Lagrangian-Hamiltonian structure and relevant conservation laws as well as some of its prototypical solutions.

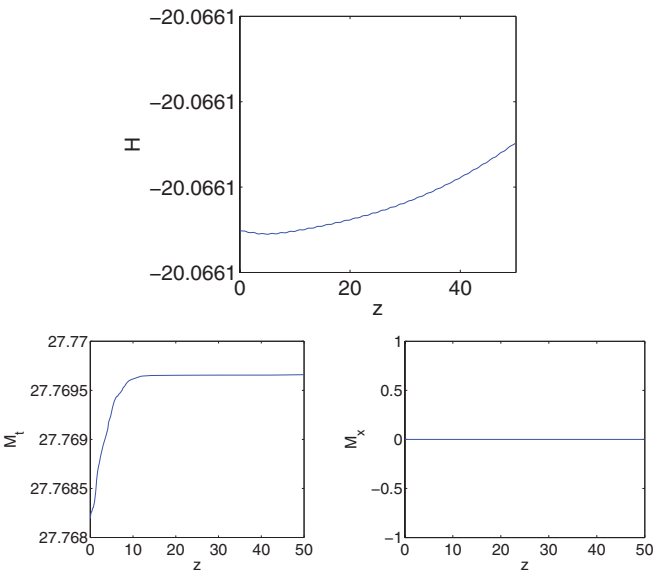

FIG. 5. (Color online) Evolution of the conserved quantities of SPE-II for the simulation shown in Fig. 4: the top panel shows the Hamiltonian H and the bottom panels show the momenta M_t (left) and M_x (right). The relative error for H and M_t is of order 10^{-4} or less, and the value of M_x is zero (and remains so throughout the simulation). All depicted quantities are dimensionless.

A. Properties and canonical structure

As in the case of the SPE-I, we integrate Eq. (28) with respect to t and, introducing the field $E = \phi_t$, we express SPE-II in the following form:

$$2\sigma(\phi_{xt} + \phi_{zt}) + \alpha\phi + s\left(\phi_t^3\right)_t = 0. \tag{29}$$

The above equation can be obtained from the variational principle, with Lagrangian density:

$$\mathcal{L} = -\frac{\alpha}{2}\phi^2 + \frac{s}{4}\phi_t^4 + \sigma(\phi_t\phi_z + \phi_t\phi_x). \tag{30}$$

The corresponding Hamiltonian can then be found as

$$\begin{aligned} H &= \int_{-\infty}^{+\infty}\int_{-\infty}^{+\infty}\left(\frac{\partial\mathcal{L}}{\partial\phi_z}\phi_z - \mathcal{L}\right)dt\,dx \\ &= \int_{-\infty}^{+\infty}\int_{-\infty}^{+\infty}\left(\frac{\alpha}{2}\phi^2 - \frac{s}{4}\phi_t^4 - \sigma\phi_t\phi_x\right)dt\,dx, \end{aligned} \tag{31}$$

while the momenta read

$$M_t = \int_{-\infty}^{+\infty}\int_{-\infty}^{+\infty}\frac{\partial\mathcal{L}}{\partial\phi_z}\phi_t dt\,dx = \sigma\int_{-\infty}^{+\infty}\int_{-\infty}^{+\infty}\phi_t^2 dt\,dx, \tag{32}$$

$$M_x = \int_{-\infty}^{+\infty}\int_{-\infty}^{+\infty}\frac{\partial\mathcal{L}}{\partial\phi_z}\phi_x dt\,dx = \sigma\int_{-\infty}^{+\infty}\int_{-\infty}^{+\infty}\phi_t\phi_x dt\,dx. \tag{33}$$

Next, we consider the Fourier transform of Eq. (28) with respect to t, which leads to the equation

$$2\sigma(i\omega)(\hat{E}_z + \hat{E}_x) + \alpha\hat{E} + s(\hat{E^3})(i\omega)^2 = 0. \tag{34}$$

Solving the above equation with respect to $\hat{E}$ we find

$$\hat{E}_z(\omega,x,z) = -\hat{E}_x - \frac{\alpha}{2\sigma(i\omega)}\hat{E} - \frac{s(i\omega)}{2\sigma}(\hat{E^3}), \text{ for } \omega \neq 0, \tag{35}$$

$$\hat{E}(\omega = 0,x,z) = 0, \text{ for } \omega \neq 0. \tag{36}$$

The latter equation leads again to the zero-mass constraint [cf. Eq. (24)] that we found in the case of the SPE-I as well. This condition will also be satisfied in our simulations below.

B. 1D breathers and initial data localized in 2D

We consider traveling wave solutions of Eq. (28), in the form $E(\xi,\eta)$, where the coordinates ξ and η are defined as

$$\xi = z, \quad \eta = t + cx - cz, \tag{37}$$

where c is an arbitrary real constant. This way, Eq. (28) is transformed to the equation

$$2\sigma E_{\xi\eta} + \alpha E + s(E^3)_{\eta\eta} = 0, \tag{38}$$

which is actually the 1D SPE model [12]. Since the latter admits breather solutions, we may follow the procedure described in the previous section and study numerically the evolution of such a 1D solution in the 2D setting of Eq. (28).

In this case also, the numerical integration of Eq. (28) has shown that this 1D solution is stable in the 2D setting (as was also in the framework of the SPE-I). An example (pertaining to parameter values $c = 0$, $s = -1/3$, $\alpha = -2$, and $\sigma = 1$) is shown in Fig. 4. Additionally, the numerical calculation of the evolution of the Hamiltonian and momenta [cf. Eqs. (31)–(33)], depicted in Fig. 5, illustrates the conservation of these quantities with a relative error of order 10^{-4} or less. We also note that similar results (not shown here) were also obtained for oblique moving breathers, i.e., for $c \neq 0$ in Eq. (37), as in the case of SPE-I.

Finally, as in the case of SPE-I, we study the evolution of localized data in 2D (i.e., in both x and t) in the framework of the SPE-II. A typical example of the result obtained by the numerical integration of Eq. (15) with such localized initial data is shown in Fig. 6 (parameter values are $s = -1/3$, $\alpha = -2$, and $\sigma = 1$). It is observed that after a small propagation distance ($z \approx 5$) the initially localized wave form begins to broaden along the t axis, but still remains localized along the x axis. As a result, a quasi-1D structure is gradually formed, which travels faster along the x direction (where it is localized) than in the t direction (where it is elongated). In the latter direction, the structure also possesses an alternating spatial structure which merits further investigation.

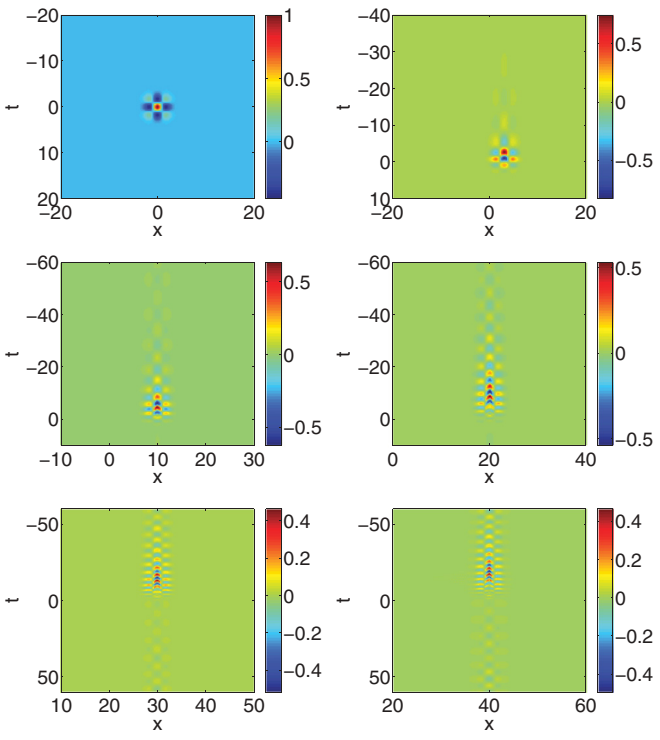

FIG. 6. (Color online) Contour plots showing profiles of the field E, in the (x,t) plane, evolved as per SPE-II, Eq. (15), with localized initial data [cf. Eq. (27)]. The snapshots, from top to bottom and left to right, correspond to $z = 0,3,10,20,30,40$. The domain for numerical computation in $x \times t$ plane is $[-20\pi,20\pi] \times [-20\pi,20\pi]$; we are zooming in here in the snapshots to show more detail. All depicted quantities are dimensionless.

V. DISCUSSION AND CONCLUSIONS

In conclusion, we have derived from Maxwell's equations two $(2+1)$-dimensional short pulse equations, referred to as SPE-I and SPE-II. These equations may find applications in various physical contexts where the study of ultrashort electromagnetic pulses is important; such contexts include nonlinear metamaterials, nonlinear optical waveguide structures, nonlinear dielectric media, and others. Since both SPE-I and SPE-II actually generalize the $(1+1)$-dimensional SPE [12], they can be used for the study of transverse (diffraction-induced) dynamics of ultrashort pulses in such settings. Suitable assumptions on the nature of the electric and magnetic field and the form of the permittivity and permeability under which the equations can be derived were provided.

We have found and presented various general properties of SPE-I and SPE-II. Particularly, we have identified the Lagrangian and Hamiltonian structure, and have used invariances to infer (from Noether's theory) the corresponding momenta, as well as the associated zero-mass constraints; the latter have to be satisfied for the solutions of these equations and, thus, are also associated with the choice of the initial data used for the numerical integration of SPE-I and SPE-II. We have conducted a series of numerical experiments for the 2D SPEs using, as initial conditions, either the 1D breather solution of the underlying 1D SPEs or a localized (in 2D) wave form—both satisfying the zero-mass constraint. Our motivation was to study the stability and transverse dynamics of the most robust solutions of the 1D analog of the system, and also examine the fate of purely 2D initial data and potentially identify structures that can be supported by the SPE-I and SPE-II models.

Our numerical simulations have shown that the 1D breathers propagate (even when they are initially perturbed by a small noise) practically undistorted. An important conclusion is that these ultrashort localized structures are actually insensitive in the presence of diffraction or, in other

words, they appear to be robust in the presence of (small) transverse perturbations for propagation distances of the order of a few hundred dimensionless units. On the other hand, simulations employing initial data localized in 2D have shown that, during evolution, the initial data gradually transforms into quasi-1D structures (which differ between SPE-I and SPE-II). In fact, we were not able to find any, purely 2D, nonlinear wave form that can be supported by either the SPE-I or the SPE-II.

The above results were obtained in the framework of the particular models, i.e., SPE-I and SPE-II, that we derived and considered in this work. It would be interesting to perform similar studies (i.e., transverse dynamics of 1D ultrashort pulses and localized 2D structures) in the framework of other versions of the SPE-I and SPE-II, stemming from the incorporation of higher-order effects (as in the 1D case, in the context of the so-called regularized SPE [23,32]). On the other hand, still in the context of SPE-I and SPE-II, it would be relevant to consider other types of solutions, e.g., loop-type solutions or periodic wave forms composed by breathers or loops (as in the spirit of the analysis in the 1D case—see Ref. [18]), and others. It would also be relevant to compare the properties of the models derived herein with those of other models for ultrashort pulses including, e.g., [2]– [11]. Finally, generalizing the present models to $(3 + 1)$ dimensions, removing the assumption of spatial homogeneity along the y direction would also constitute an interesting theme for future studies.

ACKNOWLEDGMENTS

Constructive discussions with T. P. Horikis are kindly acknowledged. The work of D.J.F. was partially supported by the Special Account for Research Grants of the University of Athens. P.G.K. gratefully acknowledges support from the National Science Foundation under Grants No. DMS-0806762 and No. CMMI-1000337 and from the Alexander von Humboldt Foundation, the Alexander S. Onassis Public Benefit Foundation, and the Binational Science Foundation.

[1] T. Brabec and F. Krausz, Rev. Mod. Phys. **72**, 545 (2000).
[2] S. A. Kozlov and S. V. Sazonov, JETP **84**, 221 (1997).
[3] I. V. Mel'nikov, D. Mihalache, F. Moldoveanu, and N.-C. Panoiu, Phys. Rev. A **56**, 1569 (1997).
[4] V. G. Bespalov, S. A. Kozlov, Y. A. Shpolyanskiy, and I. A. Walmsley, Phys. Rev. A **66**, 013811 (2002).
[5] H. Leblond and F. Sanchez, Phys. Rev. A **67**, 013804 (2003).
[6] I. V. Mel'nikov, H. Leblond, F. Sanchez, and D. Mihalache, IEEE J. Sel. Top. Quantum Electron. **10**, 870 (2004).
[7] H. Leblond, S. V. Sazonov, I. V. Melnikov, D. Mihalache, and F. Sanchez, Phys. Rev. A **74**, 063815 (2006).
[8] H. Leblond, I. V. Melnikov, and D. Mihalache, Phys. Rev. A **78**, 043802 (2008).
[9] H. Leblond and D. Mihalache, Phys. Rev. A **79**, 063835 (2009).
[10] I. V. Mel'nikov, D. Mihalache, and N.-C. Panoiu, Opt. Commun. **181**, 345 (2000).
[11] H. Leblond, D. Kremer, and D. Mihalache, Phys. Rev. A **81**, 033824 (2010).
[12] T. Schäfer and C. E. Wayne, Physica D **196**, 90 (2004).
[13] N. L. Tsitsas, T. P. Horikis, Y. Shen, P. G. Kevrekidis, N. Whitaker, and D. J. Frantzeskakis, Phys. Lett. A **374**, 1384 (2010).
[14] Y. Chung, C. K. R. T. Jones, T. Schäfer, and C. E. Wayne, Nonlinearity **18**, 1351 (2005).
[15] J. C. Brunelli, J. Math. Phys. **46**, 123507 (2005).
[16] A. Sakovich and S. Sakovich, J. Phys. Soc. Jpn. **74**, 239 (2005).
[17] A. Sakovich and S. Sakovich, J. Phys. A **39**, L361 (2006).
[18] Y. Shen, F. Williams, N. Whitaker, P. G. Kevrekidis, A. Saxena, and D. J. Frantzeskakis, Phys. Lett. A **374**, 2964 (2010).
[19] Y. Matsuno, in *Handbook of Solitons: Research, Technology and Applications*, edited by S. P. Lang and S. H. Bedore (Nova Publishers, New York, 2009).
[20] Y. Liu, D. Pelinovsky, and A. Sakovich, Dyn. Part. Diff. Eqs. **6**, 291 (2009).
[21] D. E. Pelinovsky and A. Sakovich, Commun. Part. Diff. Eqs. **35**, 613 (2010).
[22] S. A. Skobelev, D. V. Kartashov, and A. V. Kim, Phys. Rev. Lett. **99**, 203902 (2007).
[23] N. Costanzino, V. Manukian, and C. K. R. T. Jones, SIAM J. Math. Analysis **41**, 2088 (2009).
[24] S. Longhi, Waves Random Complex Media **15**, 119 (2005).
[25] D. R. Smith, W. J. Padilla, D. C. Vier, S. C. Nemat-Nasser, and S. Schultz, Phys. Rev. Lett. **84**, 4184 (2000).
[26] N. Lazarides and G. P. Tsironis, Phys. Rev. E **71**, 036614 (2005).
[27] T. P. Horikis, J. Phys. A **42**, 442004 (2009).
[28] E. Infeld, Acta Phys. Pol. A **60**, 623 (1981); E. A. Kuznetsov, M. D. Spektor, and G. E. Fal'kovich, Physica D **10**, 373 (1984).
[29] E. Infeld, A. Senatorski, and A. A. Skorupski, Phys. Rev. Lett. **72**, 1345 (1994).
[30] E. A. Kuznetsov and S. K. Turitsyn, Zh. Eksp. Teor. Fiz. **94**, 119 (1988) [Sov. Phys. JETP **67**, 1583 (1988)]; E. A. Kuznetsov and J. J. Rasmussen, Phys. Rev. E **51**, 4479 (1995).
[31] D. E. Pelinovsky, Yu. A. Stepanyants, and Yu. S. Kivshar, Phys. Rev. E **51**, 5016 (1995).
[32] V. Manukian, N. Costanzino, C. K. R. T. Jones, and B. Sandstede, J. Dyn. Diff. Eq. **21**, 607 (2009).